J. Fluid Mech. (1968), *vol.* 32, *part* 4, *pp.* 705–720
Printed in Great Britain

Experiments on the pressure drop created by a sphere settling in a viscous liquid. Part 2. Reynolds numbers from 0·2 to 21,000

By GUILI A. FELDMAN† AND HOWARD BRENNER‡
Department of Chemical Engineering, New York University

(Received 4 October 1967)

The pressure drop ΔP created by the motion of a 'small' spherical particle settling along the axis of a large-diameter circular cylinder filled with a quiescent liquid was measured in the particle Reynolds number range (based on diameter) from $Re = 0{\cdot}2$ to 21,000. For $Re < 125$ it was found that $\Delta PA/D = 2{\cdot}0$ (A = cylinder cross-sectional area; D = particle drag), in agreement with existing theory in the Stokes and Oseen regimes. Beyond $Re = 125$ a fairly abrupt transition occurs, the $\Delta PA/D$ ratio decreasing asymptotically towards 1·0, the limiting value predicted by elementary momentum principles for an 'unbounded' fluid, with increasing Re. At $Re \approx 6000$ the transition is essentially complete.

1. Introduction

A previous paper (Pliskin & Brenner 1963; hereafter referred to as part 1) reported the results of experimental measurements of the pressure drop caused by the vertical settling motion of a single spherical particle of radius a along the axis of a long circular cylinder of radius R_0 ($a/R_0 \ll 1$) filled with viscous fluid, for particle Reynolds numbers Re up to about 1·6 ($Re = 2aU/\nu$; U = sphere terminal settling velocity, ν = kinematic viscosity). This pressure drop refers to the limiting dynamic pressure difference between any two sufficiently distant horizontal planes on each side of the sphere, the pressure being greatest on that plane towards which the sphere advances. The motivation for the original experiments arose from the theoretical prediction (Brenner 1962) that, in the Stokes and Oseen regimes, i.e. $Re < 2$, the pressure drop force, ΔPA ($A = \pi R_0^2$), would not simply be equal to the drag force D on the sphere in the 'unbounded' limit $a/R_0 \to 0$ (as might otherwise be implied by elementary momentum arguments) but rather would be given by the relation

$$\Delta PA/D = 2 \tag{1}$$

for motion along the cylinder axis.

Equation (1) was adequately confirmed in part 1 for the limited region investigated, $0{\cdot}1 < Re < 1{\cdot}6$ (and $0{\cdot}04 < a/R_0 < 0{\cdot}25$). It was further sug-

† Present address: UniRoyal Inc., Research Center, Wayne, New Jersey 07470.

‡ Present address: Department of Chemical Engineering, Carnegie–Mellon University, Pittsburgh, Pennsylvania 15213.

gested on theoretical grounds (Brenner 1962), and indicated by the general trend of the experimental data, that (1) might be valid even at Reynolds numbers substantially beyond $Re = 2$, at which point both the Stokes and the Oseen drag formulas cease being accurate. For, unlike the drag, which depends upon the detailed flow field in the immediate proximity of the particle, the pressure drop depends only upon the nature of the flow at relatively great distances from the particle, especially in the neighbourhood of the cylinder walls, where the no-slip boundary condition is crucial to the validity of (1). And there, because the disturbance created by the sphere's motion has been effectively attenuated over the relatively enormous distances involved, at least in the limit where $a/R_0 \to 0$, the fluid is virtually at rest. It is entirely conceivable, therefore, that (1), though derived by making the usual assumption of small inertial effects implicit in the Stokes and Oseen drag laws, may have a range of applicability greatly exceeding $Re = 2$. It is with the experimental confirmation of this hypothesis that the present paper is primarily concerned, as well as with establishing the asymptotic law governing the $\Delta PA/D$ *vs.* Re relationship as $Re \to \infty$, if indeed one exists.

Experiments are described herein covering the Reynolds number range from 0·2 to 21,000. The greatly extended Re range investigated here, compared with that of part 1, was made possible by the use of a sensitive, electronically monitored, rapid-response, differential pressure transducer in place of the U-tube micromanometer employed in part 1. A more detailed description of the experimental programme than is described in the sequel is available elsewhere (Feldman 1967).

2. Equipment and experiments

Major pieces of apparatus and auxiliary equipment are depicted schematically in figure 1. The main components consisted of: (i) a vertical glass pipe, 10 ft. long and 6·03 in. inside diameter, in which the spheres were allowed to settle; (ii) a vertical brass pipe, 10 ft. long and 2 in. nominal diameter, connected at its base to the glass column, and used to balance the hydrostatic pressure in the main column; (iii) a differential pressure transducer, with its two pressure ports joined by tubing to openings at the tops of the glass and brass pipes, respectively; (iv) a variable, high-speed, strip-chart recorder, used to record permanently the electrical signal issuing from the transducer amplifier.

Except for the transducer controller and recorder, the entire apparatus was housed within a large, temperature-controlled, Masonite chamber with a Plexiglass door. Temperature control within the enclosure housing the apparatus was achieved by re-circulating air from a constant environment chamber. Both columns were filled with the appropriate liquid being tested to within a few inches of their tops. The remainder of the system contained air at essentially atmospheric pressure, serving to transmit to the transducer the pressure difference created by the sphere's motion through the liquid. The system consisting of the main column, balancing column, inter-connexion, and transducer constituted an air-tight assembly, completely isolated from possible atmospheric fluctuations during the course of a single experiment.

Five different liquids were utilized to achieve the desired Reynolds number range. These consisted of various mixtures (from 0 to 100%) of water and a highly viscous, water-soluble, commercial lubricant, UCON 50-HB-5100 (Union Carbide). The Newtonian character of the UCON fluid had already been

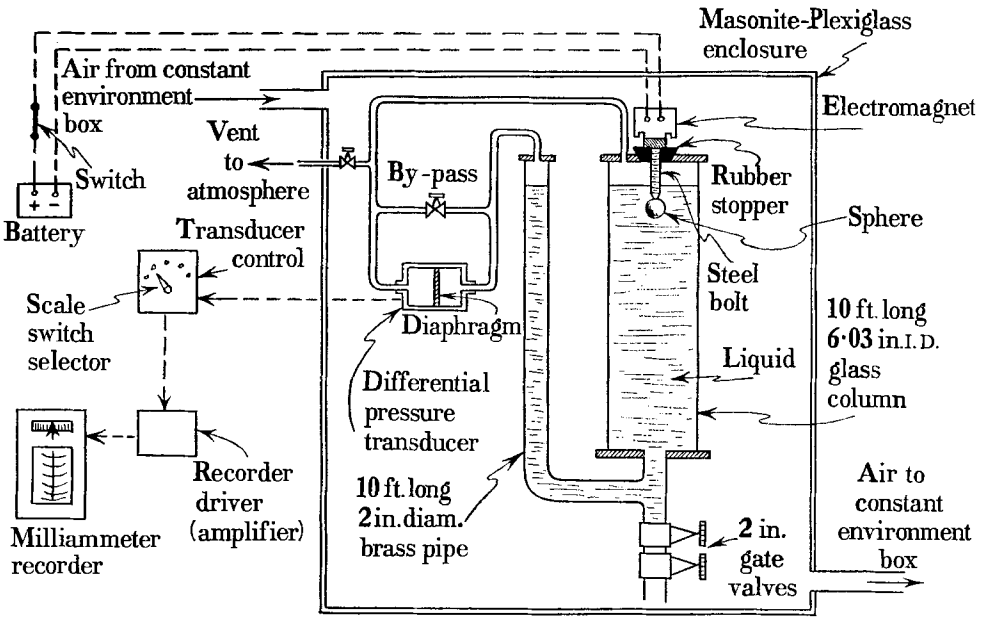

FIGURE 1. Diagram of apparatus.

	Temperature (°C)	Fluid *A* 100 wt.% UCON	Fluid *B* ≈ 53 wt.% UCON	Fluid *C* ≈ 32 wt.% UCON	Fluid *D* ≈ 20 wt.% UCON	Fluid *E*† distilled water
ρ, g/ml.	23	—	—	—	1·024	—
ν, centistokes	23	—	—	—	10·93	—
ρ, g/ml.	24	1·050	—	—	—	0·9973
ν, centistokes	24	2243	—	32·4	10·55	0·9167
ρ, g/ml.	25	1·048	1·061	—	1·023	0·9971
ν, centistokes	25	2098	—	31·0	10·16	0·8963
ρ, g/ml.	26	1·046	—	—	—	—
ν, centistokes	26	1967	199·1	—	—	—
ρ, g/ml.	27	—	1·060	—	—	—
ν, centistokes	27	—	189·1	—	—	—

† Properties abstracted from Perry (1963).

TABLE 1. Measured physical properties of UCON–water solutions employed

established in part 1. Relevant properties of the various liquid mixtures at the temperatures employed in the experiments are tabulated in table 1, ρ being the fluid density.

Two classes of spheres were employed in the experiments: (i) precision steel ball bearings with true diameters ranging from $\frac{3}{16}$ to $\frac{5}{8}$ in., having tolerances of the order of a few ten-thousandths of an inch; (ii) composite polyethylene–steel

spheres of 1·5 and 3 in. nominal diameters, constructed by drilling incompletely-penetrating holes of different diameters on each side of an axis of the solid polyethylene sphere, and inserting a tightly fitting cylindrical steel plug with a T-shaped cross-section. Fine adjustments of the mean density of the composite sphere were made either by machining the steel plug or by inserting lead shot into the air gap between the base of the steel plug and the interior of the sphere. Departures from sphericity due to the flattened ends of the plug were negligible.

Individual spheres were released at the axis of the liquid-filled glass column after having been held in place beneath the surface by an electromagnet controlled from outside the sealed system. Release of a sphere caused the liquid level to fall in the larger column and rise in the smaller one until they reached their equilibrium heights appropriate to the pressure difference generated by the sphere's steady motion. Sphere settling times ranged from about 1·8 to 50 sec.

The principal experimental difficulty resided in accurately measuring and recording these minute pressure differences, which ranged from about 0·021 to 1·5 mm of water during the investigation. The instrument utilized was a Model 1004A Sensitive Differential Pressure Transducer (Monroe Electronics, Middleport, New York), consisting essentially of a grounded aluminium diaphragm under radial tension with a capacitor plate positioned on either side of the diaphragm, and a preamplifier. This was connected to a Model 117A Sensitive Differential Pressure Transducer Control and Indicator (Monroe), consisting of an amplifier and a 4 kc sinusoidal oscillator. The latter excited the transducer in a Wheatstone bridge configuration. Diaphragm displacement produced a bridge imbalance, giving rise to an error voltage which varied linearly with the pressure difference applied across the diaphragm. Seven differential pressure ranges were provided: 0 to 0·1, 0·2, 0·5, 1·0, 2·0, 5·0 and 10·0 mm of water at full scale. Sensitivity of the transducer was about 0·0005 mm of water (on the lowest scale). The transducer control provided a recorder output jack delivering a 50 μA signal for any full-scale diaphragm deflexion to a Model 213D 1·5 mA Recorder Driver (Monroe) which amplified the signal by a factor of 30. This amplified signal was fed into a Model A 601 C Recording DC Milliammeter (Esterline–Angus Instrument Co., Indianapolis, Indiana), which is a strip-chart recorder with a full range of $-1{\cdot}5$ mA to 0 to $+1{\cdot}5$ mA. The recording pen had a response time of about 1 sec for full-scale deflexion. This was the limiting factor with regard to instrument response time, since the diaphragm itself had a response time of only about 10 millisec. In order to furnish an adequate record of pressure difference *vs.* time for different sphere-settling velocities, the strip-chart recorder was provided with a wide range of possible chart speeds, from $\frac{3}{4}$ in./h to 3 in./sec.

Though an approximate calibration of the differential pressure transducer was furnished by the manufacturer, based upon his calibration of the 0–10 mm scale in conjunction with the assumed linearity of the diaphragm response, it was deemed advisable to recalibrate the instrument. Accurately known pressure differences as small as 0·07 mm of water were generated across the transducer by the simple technique illustrated in figure 2. Two 8-litre (approx.) glass bottles, initially containing air at atmospheric pressure, and immersed in a stirred water

trough to maintain them at isothermal conditions, were attached by tubing to the pressure inlets on either side of the transducer. One of the bottles also led to a mercury-filled burette of either 2 ml. or 50 ml. capacity, depending upon which of the seven available transducer scales was being calibrated. Prior to applying any pressure difference the volumes of the glass bottles, connecting tubing, etc., on each side of the diaphragm were accurately measured, and the uniform pressure in each noted by means of a barometer. With the by-pass valve and atmospheric vent closed, a measured volume of mercury was released from the burette, collected in a weighing bottle, and weighed on an analytical balance to furnish a more accurate measurement of its volume than provided by the graduations on the burette. Since the mass and temperature of the air in each of the two closed subsystems on either side of the diaphragm remained constant, the increase in volume caused by removal of mercury from one of the subsystems was converted into an equivalent pressure difference by application of the ideal gas law. An approximate method for measuring the small volume changes in each of the two subsystems due to diaphragm movement was incorporated into the calculation (Feldman 1967), though this refinement resulted in only a very minor correction. Due to the essentially adiabatic expansion of the air occurring immediately upon release of the mercury, it was found necessary to wait about 2·5 min for the system to return to isothermal conditions, as attested to by the fact that the pressure difference across the diaphragm no longer changed with time.

The calibration procedure was repeated for all seven transducer scales except the 5 mm one. The ΔP calibration obtained in this manner differed from the manufacturer's by about 10–20 %, which lies somewhat beyond the 5 % accuracy range at full scale claimed (but not guaranteed). However, in view of the obvious uncertainties in the manufacturer's calibration technique, especially in the lower ΔP range, the discrepancy was not regarded as casting any doubt on the validity of our procedure. Strong evidence of the high accuracy of our calibration was indirectly furnished by the fact that the theoretical pressure drop, cited in (1), was experimentally confirmed to within about 3 % in the *Re* range where it would normally be expected to be applicable.

The calibration procedure outlined above was repeated periodically throughout the course of the experiments with satisfactory reproducibility. Because the transducer was found to be slightly humidity sensitive, it was stored in a desiccator until just prior to use.

In order to interpret the data from the sphere-dropping experiments, elementary manometric principles were employed to relate the pressure difference observed across the diaphragm to the true pressure drop incurred by the sphere's motion. These quantities are not precisely equal, owing to a number of minor corrections emanating from various sources. However, in our experimental configuration, the difference between these two quantities was calculated to be only 2·0 %.

A characteristic feature of both the calibration runs and experiments utilizing the most sensitive transducer scales was a drift in the 'zero' reading of the pressure differential across the transducer. (In the case of the experimental runs

see the lower lines in figures 3*a*, 3*b* and 3*c*.) This drift occurred after the atmospheric vent and by-pass in figure 1 were closed, but before the sphere was released. No drift was observed when both sides of the system were vented to the atmosphere. This phenomenon was previously reported in part 1, where it was tentatively attributed to non-uniformities in liquid density due to inadequate temperature control; however, it is actually due to minute temperature variations in the two air volumes transmitting the pressures to each side of the transducer. A simple application of the ideal gas law shows that the existence of a temperature difference as small as 0·001 degF between these two air volumes after the intercommunication is closed would create a pressure differential of about 0·02 mm water, which is approximately equal to the magnitude of the smallest pressure difference arising in the experiments.† Fortunately, however, because the drift rate remained sensibly constant during the brief duration of an experiment,‡ the same drift rate as was observed in the 'zero' readings at the beginning and end of an experiment was also visibly discernible in the pressure drop readings themselves during the course of the experiment.§ Hence the pressure drop could be accurately obtained by subtracting the hypothetical 'zero' reading, obtained by interpolating the 'before' and 'after' zero readings (the dotted lines in the lower portions of figures 3*a*–3*c*), from the corresponding pressure reading *at the same instant of time*. Because of the linearity of the drift with time, this difference was independent of time. Hence the drift had but a minimal effect on the accuracy of the experimental measurements.||

† Since, according to the ideal gas law, $\Delta p/p = \Delta T/T$, where Δp is the change in pressure p resulting from a change, ΔT, in the absolute temperature T, it would seem desirable in any future work to investigate the use of a pressure p considerably below atmospheric (but, of course, above the vapour pressure of the liquid) in order to effect a proportional reduction in the pressure drift Δp for a given temperature drift ΔT.

‡ Because of its heating and cooling cycles, the re-circulated air issuing from the constant environment chamber (figure 1) would produce a sinusoidal rate of drift (of undesirably large amplitude) if left functioning during the experiments. Therefore, immediately prior to sphere release, the constant environment chamber and air blowers (used to re-circulate the temperature-controlled air) were shut down. Since the temperatures in the ambient atmosphere and enclosure were always very nearly the same, the temperature within the enclosure would always respond in the same manner to this sudden change; moreover, this response was slow. As a consequence, the drift always occurred in the same direction, as illustrated in figures 3*a*, 3*b* and 3*c*, and was practically linear over relatively short periods of time. Over longer times, the drift rate increased. Accordingly, spheres were released as quickly as possible after interruption of the air flow from the constant environment chamber. With this precaution, the drift rate could be made as small as 0·001 mm of water per minute.

§ The existence of *continuous* records of these quantities confirms, incidentally, the *assumption* in part 1 of equality of drift rates.

|| The same was not true for the calibration runs however, even though the origin of the phenomenon is identical. Drift occurred after the atmospheric vent and by-pass (figure 2) were closed, but before release of the mercury. The drift here could not be made to behave linearly, nor at a small rate. Interruption of the stirring caused linear drift (see previous footnote), but at an excessively large rate considering that it was necessary to wait 2·5 min after the mercury release until equilibrium conditions prevailed. This drift therefore constituted the major limitation in accurately calibrating the most sensitive transducer scales. The highest rate of drift observed during calibration was about 0·002 mm of water per minute.

Inspection of the strip-chart ΔP *vs.* t (t = time) record rendered it possible to ascertain whether the sphere's settling time through the column had been sufficient to attain a steady-state pressure differential. This 'response time' (see figures 3*a*–3*c*) varied appreciably with Re. For example, it was found to be about 3 sec for $Re = 2{\cdot}4$, increasing to about 15 sec at $Re = 123$, and subsequently decreasing to 1·3 sec at $Re = 5720$. As a result, it was possible to use the small, fast-settling,† steel spheres at the smaller and larger Reynolds

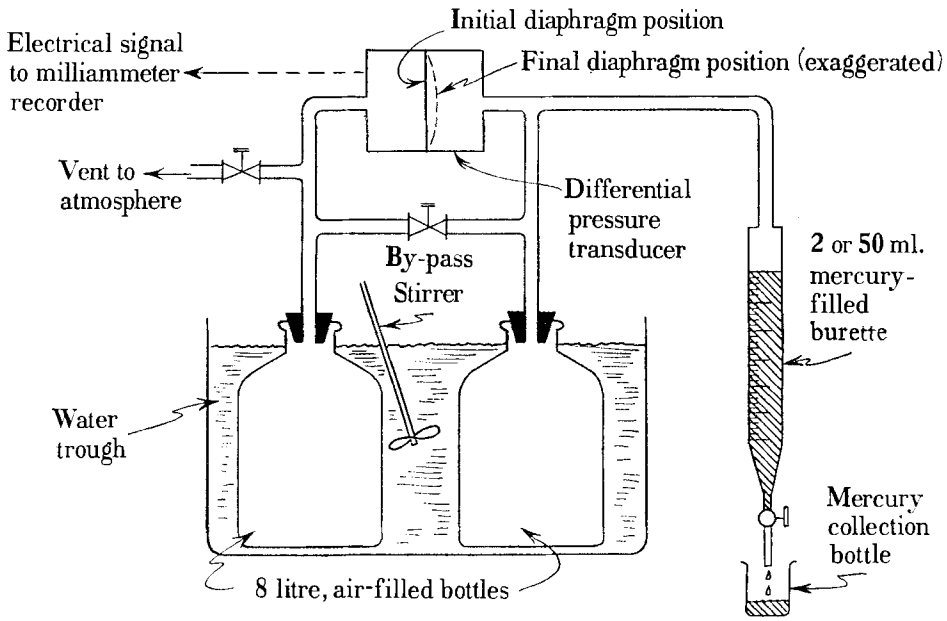

FIGURE 2. Calibration procedure.

numbers, but not in the intermediate range from about $Re = 60$ to 700, where it was necessary to resort to the larger, slower-settling, plastic–steel spheres. In order to obtain pressure drops which would not be excessively small, and therefore outside the realm of accurate measurement, the smaller settling velocities of the composite spheres were partially compensated for, insofar as increasing the drag force for a specified settling velocity, by resorting to much larger sphere diameters ($a/R_0 = 0{\cdot}25$–$0{\cdot}5$) than were utilized for the steel spheres ($a/R_0 \leqslant 0{\cdot}1$). Possible wall effects thereby incurred are discussed in §3.2.

3. Results and conclusions

3.1. *Experimental results*

The steady-state drag force D on each steel sphere falling in a specified liquid was computed by subtracting the calculated buoyant force exerted on it by the appropriate liquid from the measured weight of the sphere (in air). This procedure was not sufficiently accurate for the polyethylene–steel spheres; here the

† Faster-settling spheres experience larger drags, thereby giving rise to larger, more accurately measurable, pressure drops.

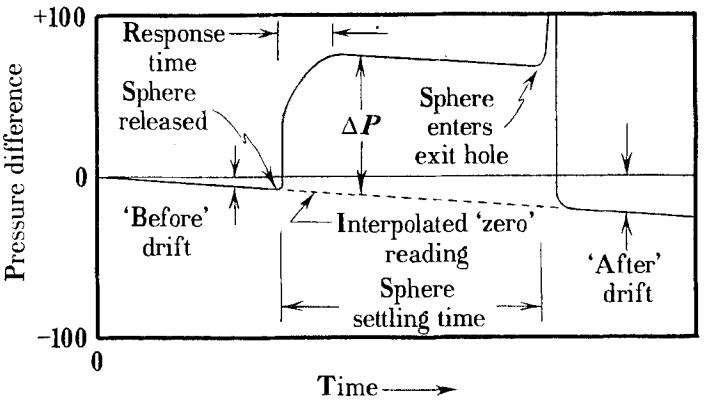

FIGURE 3*a*. General features of a typical strip-chart record for $Re < 300$.

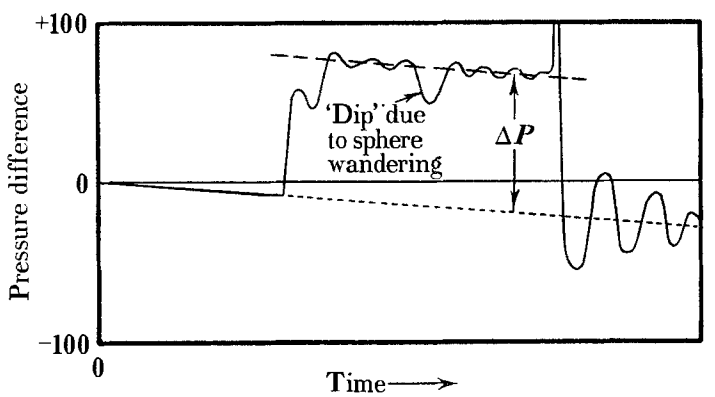

FIGURE 3*b*. General features of a typical strip-chart record for $300 < Re < 6000$.

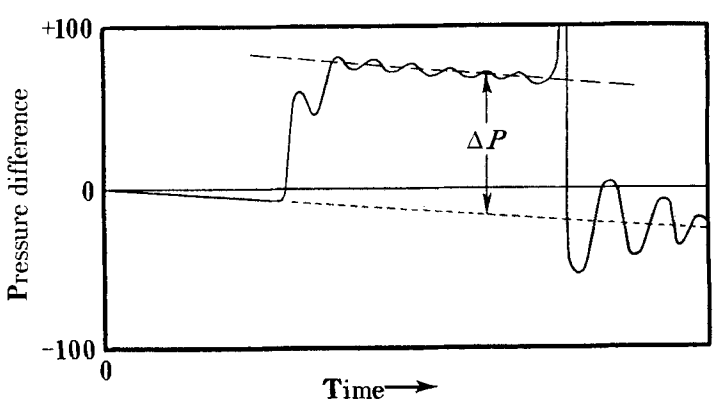

FIGURE 3*c*. General features of a typical strip-chart record for $Re > 6000$.

drag was directly measured by weighing the sphere in a sample of the liquid in which it was ultimately to be released. The results of both classes of weighings are recorded in table 2, along with a specification of the sphere size and liquid involved in each group of replicate experiments.

Expt. group number	Fluid (temperature, °C)	Sphere diameter, $2a$ (in.)	Sphere weight in air (g)	Sphere weight in fluid (g)	Drag D (g)	True terminal settling velocity, U (ft./sec)	True† pressure drop, ΔP (mg/cm²)
I	*A* (25·4°)	$\frac{1}{4}$	1·045	—	0·904	0·214	9·57
II	*A* (25·3°)	$\frac{9}{32}$	1·485	—	1·285	0·265	13·6
III	*A* (25·3°)	$\frac{13}{32}$	4·475	—	3·871	0·508	41·1
IV	*A* (25·3°)	$\frac{17}{32}$	10·013	—	8·663	0·788	91·1
V	*A* (25·4°)	$\frac{5}{8}$	16·326	—	14·13	1·03	149
VI	*B* (26·1°)	$\frac{7}{32}$	0·698	—	0·603	1·06	6·51
VII	*B* (27·0°)	$\frac{9}{32}$	1·485	—	1·283	1·49	14·3
VIII	*B* (26·7°)	$\frac{13}{32}$	4·473	—	3·863	2·27	42·9
IX	*B* (27·0°)	1·5	—	8·662	8·662	1·00	97·9
X	*C* (24·6°)	1·5	—	0·644	0·644	0·334	6·83
XI	*C* (24·2°)	1·5	—	1·994	1·994	0·707	18·4
XII	*C* (24·4°)	1·5	—	3·845	3·845	1·01	31·7
XIII	*C* (24·5°)	3	—	12·445	12·445	0·675	84·6
XIV	*C* (24·9°)	1·5	—	12·231	12·231	1·95	77·6
XV	*D* (23·5°)	$\frac{9}{32}$	1·484	—	1·289	3·59	7·84
XVI	*D* (24·3°)	$\frac{11}{32}$	2·713	—	2·357	4·10	13·8
XVII	*D* (24·6°)	$\frac{15}{32}$	6·870	—	5·965	5·12	36·1
XVIII	*D* (24·4°)	$\frac{5}{8}$	16·329	—	14·18	5·82	82·2
XIX	*E* (25·0°)	3	—	1·270	1·270	0·195	7·29
XX	*E* (25·0°)	$\frac{3}{16}$	0·439	—	0·383	3·53	2·11
XXI	*E* (24·0°)	$\frac{9}{32}$	1·485	—	1·295	3·85	6·76
XXII	*E* (24·0°)	$\frac{3}{8}$	3·522	—	3·072	4·47	16·4
XXIII	*E* (24·0°)	3	—	14·851	14·851	0·718	85·5
XXIV	*E* (24·0°)	$\frac{1}{2}$	8·356	—	7·290	5·08	40·9

† 1 mm water = 100 mg/cm².

TABLE 2. Averaged experimental data

Three to five replicate experiments were made of the dynamic pressure difference, ΔP, and of the terminal settling velocity U through the 10 ft. (approx.) column for each data point (i.e. same sphere, liquid, and temperature). The arithmetic averages of ΔP and U for each series of replicate experiments, represented by a Roman numeral in the table, are recorded in table 2. In conjunction with other data tabulated in tables 1 and 2, these averages were employed to compute the corresponding values of $\Delta PA/D$ ($A = 28{\cdot}6$ in.²) *vs.* $Re = dU/\nu$ ($d = 2a$), tabulated in table 3.

The settling times of many spheres were as small as 2 sec, making it impractical to use a stop watch for the determinations. Measurement of the settling velocity was therefore based upon the strip-chart record of ΔP *vs.* t.

Simultaneous with sphere release, a sudden initial rise in the pressure differential occurred. Upon entering the small exit hole at the inlet to the sphere recovery valve located at the base of the column, the ΔP value underwent a second sudden rise (due to the reduction in cross-sectional area), before reverting to its zero-point reading upon coming to rest. Typical strip-chart records at various

Experiment group number	a/R_0	Re	$\Delta PA/D$
I	0·041	0·204	1·95
II	0·047	0·284	1·95
III	0·067	0·76	1·96
IV	0·088	1·55	1·94
V	0·104	2·36	1·94
VI	0·036	9·1	1·99
VII	0·047	17·2	2·05
VIII	0·067	37·3	2·05
IX	0·25	61·5	2·08
X	0·25	123	1·96
XI	0·25	258	1·70
XII	0·25	370	1·52
XIII	0·50	495	1·25
XIV	0·25	730	1·17
XV	0·047	730	1·12
XVI	0·057	1,050	1·08
XVII	0·078	1,800	1·12
XVIII	0·104	2,710	1·07
XIX	0·50	5,060	1·06
XX	0·031	5,720	1·02
XXI	0·047	9,140	0·96
XXII	0·062	14,200	0·98
XXIII	0·50	18,100	1·06
XXIV	0·083	21,400	1·03

TABLE 3. Calculated experimental results

Reynolds numbers are shown in figures 3*a*–3*c*. Reproducibility of the settling-time measurements in replicate experiments was generally within 1–2 %, even when the time of fall was as small as 2 sec. Knowledge of the exact length of sphere travel through the column, the distance between the two abrupt pressure rises on the strip-chart, and the recorder chart speed, then yielded an average settling velocity. This value is somewhat less than the true terminal velocity U, owing to the time required to accelerate the sphere to its ultimate terminal velocity from its initial rest position. Based upon the approximate dynamics of unsteady settling under the influence of a constant external force (Lapple & Shepherd 1940), the true terminal velocity was then calculated by applying an appropriate correction factor for each experimental condition. The corrections were relatively small, amounting to only 9 % in the worst case. It is these corrected values which are reported in table 2.

After correcting for wall effects (McNown *et al.* 1948; Haberman & Sayre 1958; Fidleris & Whitmore 1961), the Reynolds number/drag coefficient relationship implicit in the data reported in the tables was in good agreement with accepted values (Lapple & Shepherd 1940) for all but two data points.† Excluding these two points, the standard deviation of the drag coefficient from accepted values was about 6 %, the maximum deviation being 13 %. These small discrepancies are due primarily to uncertainties in the viscosity arising from small temperature gradients within the column, possible errors in measuring the small settling-time intervals, uncertainties in the proper settling-velocity corrections arising from the acceleration phase of the sphere's motion, and unstable sphere motions (see §3.3) observed at $Re > 300$. Since an accurate knowledge of Re was not critical to the investigation, no attempts were made to secure more reliable measurements of this parameter.

For Reynolds numbers less than about 700, interpretation of the ΔP *vs.* t strip-chart record was relatively straightforward. However, for $Re > 700$ the response of the column of liquid to the suddenly applied pressure difference was highly underdamped, as indicated by the oscillations in the $(\Delta P, t)$ curves in figures 3*b* and 3*c*. Consequently, an absolutely steady-state ΔP value could not be obtained during the few seconds of settling time available. However, except for the existence of sudden 'dips' (figure 3*b*), whose significance is discussed in §3.3, and taking into account the drift, the ΔP value oscillated about an obvious mean value. This made it possible to secure a hypothetical steady-state ΔP value by drawing a smooth curve through the centres of the sinuous $(\Delta P, t)$ curves. These correspond to the dashed curves in the upper portions of figures 3*b* and 3*c*, which are seen to lie parallel to the interpolated zero-point curves.

The reproducibility of replicate ΔP measurements was surprisingly good, especially for $Re < 300$, corresponding to stable settling (see §3.3), where standard deviations were less than 1 % of the average value. But, even at higher Reynolds numbers, where settling was unstable, the largest standard deviation encountered in replicate experiments was only 2·2 % of the average. Because of the considerable accuracy of the measurements of D and A, this same degree of reproducibility is equally applicable to the dimensionless grouping $\Delta PA/D$ in table 3. On the other hand, due primarily to uncertainties in calibration, the accuracy of the $\Delta PA/D$ measurements is only estimated to be between 3 and 8 %, the more accurate figure cited being applicable to the lower Reynolds number data, where settling was stable and response of the column liquid was overdamped.

A plot of $\Delta PA/D$ *vs.* Re, based on the tabulation in table 3, is presented in figure 4. It will be seen that $\Delta PA/D = 2{\cdot}0$ for $Re < 125$, and that $\Delta PA/D = 1{\cdot}0$ for $Re > 6000$, though the latter Reynolds number is subject to large uncertainty. In the intermediate range, $125 < Re < 6000$, the pressure drop force/drag ratio undergoes an apparently rapid transition between these two extreme limits.

† Unstable sphere motion in conjunction with retardation of settling due to repeated collisions with the cylinder walls is probably responsible for the large discrepancies (about 40 %) observed in the case of the two runs at $Re = 5060$ and 18,100 with 3 in. spheres.

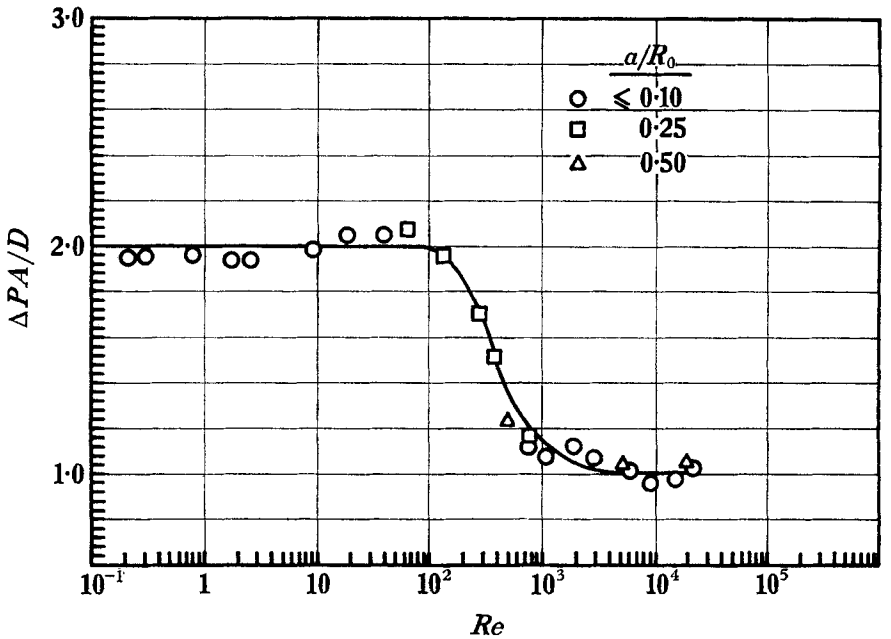

FIGURE 4. Pressure drop force/drag ratio *vs.* particle Reynolds number.

3.2. *Wall effects*

The various sphere sizes employed in the experiments encompassed the range of sphere–cylinder radius ratios from $a/R_0 = 0{\cdot}03$ to $0{\cdot}5$, though two-thirds of the total number of experiments conducted lay in the range $a/R_0 \leqslant 0{\cdot}10$. For a sphere falling along the axis of a circular cylinder in the Stokes regime, the effect of the wall upon the $\Delta PA/D$ ratio is (Brenner 1966)†

$$\Delta PA/D = 2[1-\tfrac{2}{3}(a/R_0)^2]+O(a/R_0)^3, \tag{2}$$

where D refers to the drag on the sphere, including wall effects. For values of $a/R_0 \leqslant 0{\cdot}10$, the wall correction is less than $0{\cdot}7\,\%$, and therefore negligible, at least in the Stokes regime. It is well known that the effect of a cylindrical boundary upon the *drag* experienced by a spherical particle moving along its axis decreases rapidly with increasing Re for a fixed a/R_0 (McNown *et al.* 1948; Fidleris & Whitmore 1961). The present experiments indicated that $\Delta PA/D$ behaves in a similar manner. For example, at $Re = 730$, table 3 shows that the $\Delta PA/D$ values at $a/R_0 = 0{\cdot}047$ and $0{\cdot}25$ differ by less than $5\,\%$, which lies within the limits of accuracy of the data. Similar implications arise by comparing the data points for the significantly different sphere sizes in the Reynolds number ranges 5060 to 5720 and 18,100 to 21,400.‡

† The comparable result for a non-axially situated sphere is (Brenner 1966)

$$\Delta PA/D = 2[1-(b/R_0)^2-\tfrac{2}{3}(a/R_0)^2]+O(a/R_0)^3,$$

where b is the distance of the sphere centre from the cylinder axis.

‡ In addition to these data, further (preliminary) experiments conducted with a 1 in. diameter composite sphere at $Re \approx 60$ yielded the same $\Delta PA/D$ value, to within the experimental uncertainty, as noted in table 3 for the 1·5 in. sphere at $Re = 61{\cdot}5$.

It seems consistent to conclude therefore that conventional wall effects were negligible in all experiments reported here, even for those in which a/R_0 was as large as 0·5.

3.3. *Unstable sphere movement*

At $Re < 300$ the spheres settled stably, their motion being purely vertical, along the cylinder axis. However, for $Re > 300$ the spheres were observed to 'wobble' (i.e. an imaginary axis fixed in the sphere would rock to-and-fro), and 'wander' (i.e. the sphere centre moved off the cylinder axis, occasionally meandering so far as to strike the wall). In most cases of instability the sphere centre performed a sinuous wandering about a mean position at the cylinder axis. However, in a few cases the wandering motion was of such an extreme nature that the sphere, upon approaching the wall, remained permanently in its proximity as it settled, rather than returning to the cylinder axis. In general, for the same Re, the denser spheres displayed less wandering. These unstable motions are caused by an increasing instability of the fixed-ring vortex in the wake of the sphere with increasing Reynolds number.†

Proper interpretation of the pressure drop data in the presence of wandering requires further discussion. In the general case, a momentum balance taking account of all external forces exerted on the fluid within the column yields (Brenner 1962)

$$\Delta PA/D = 1 + (F_w/D), \tag{3}$$

where F_w is the net shearing force exerted by the vertical cylinder walls on the liquid. Now, in both the Stokes and Oseen regimes, the wall force due to the motion of a small, non-axially situated particle within a circular cylinder is (Brenner 1962)

$$F_w/D = 1 - 2(b/R_0)^2 \tag{4}$$

correctly to terms of $O(a/R_0)^2$, where b is the distance of the particle centre from the cylinder axis. Substitution into (3) yields

$$\Delta PA/D = 2[1 - (b/R_0)^2], \tag{5}$$

which shows that the pressure drop varies with the eccentric location, b/R_0, of the sphere centre within the cylinder, at least at small Re.

For $Re > 6000$ the strip-chart record of ΔP *vs.* t (see figure 3*c*) revealed no apparent changes in pressure drop as the sphere wandered about to different eccentric locations. Thus, in this Reynolds number range, ΔP is essentially independent of eccentricity. Since D, being the net weight of the sphere, is necessarily independent of eccentricity, (3) indicates that F_w is also independent of b/R_0. In fact, since figure 4 indicates that $\Delta PA/D = 1{\cdot}0$ in this Re range, it follows that $F_w = 0$ at all eccentric positions. This inference is consistent with all of the experimental data obtained at the higher Reynolds numbers.

† According to Taneda (1956) a closed re-circulating wake, that is, a standing eddy, first makes its appearance at $Re \approx 10$. At $Re \approx 130$ the flow starts to become unsteady, with oscillations of the downstream part of the wake. Above $Re \approx 200$, the flow becomes irregular, with separation of the fixed-ring vortices from the rear of the sphere, followed by the subsequent formation of new ones. More complete details are critically summarized by Torobin & Gauvin (1959).

In the region $300 < Re < 6000$ the $\Delta PA/D$ ratio was found to be greater than 1·0 but less than 2·0. In accordance with (3) this indicates that F_w is not zero. Moreover, by analogy to (4), F_w probably depends upon b/R_0, though perhaps much more weakly than is true of (4), which applies only at small Reynolds numbers. Consequently, (3) requires that $\Delta PA/D$ vary with eccentricity too. This dependence upon b/R_0 seems to be confirmed by records of ΔP *vs.* t (see figure 3*b*), where sudden 'dips' in the ΔP value probably correspond to off-axis sphere wandering.† In such cases the maximum steady-state ΔP reading was assumed to correspond to the value appropriate to axial motion. This interpretation is consistent with the fact that no 'dips' were observed for $Re > 6000$ (despite the off-axis wandering), in which region the pressure drop is presumably independent of eccentricity.

Despite the bizarre and complex appearance of many of the strip-chart records obtained at the higher Reynolds numbers, occasioned by such factors as the initial and final unsteadiness of the system response, the drift, the wobbling, the wandering, and the underdamped nature of the system response, the individual ΔP *vs.* t records for replicate experiments were so impressively alike—even in finest details—as to be superposable, one on the other. They were as characterististic of a given system as an infra-red spectral record is of a specified compound.

4. Discussion

The principal results of the present series of experiments are contained in figure 4. It appears, *inter alia*, that the pressure drop force/drag ratio for a spherical particle settling along the axis of a circular tube is accurately given by $\Delta PA/D = 2{\cdot}0$, in accordance with theory (Brenner 1962), for particle Reynolds numbers less than about 125. More precisely, the ten data points comprising the region $0{\cdot}20 < Re < 123$ furnish an average value of $\Delta PA/D = 1{\cdot}99$ with a standard deviation of about 2·5% from the average. This corroborates and extends the conclusions of part 1. In particular, the present experiments show that the theory governing (1) is valid for Reynolds numbers substantially greater than $Re \approx 2$, the value commonly accepted as the upper limit of validity of the Stokes and Oseen drag laws for a sphere (Maxworthy 1965).

In view of the underlying theoretical analysis, such agreement carries with it the implication that (5), which applies more generally to an off-centre sphere, would also be valid in essentially the same Reynolds number range, provided that conventional wall effects were absent, and that such asymmetric motions were stable.‡ Similar implications exist for cylindrical boundaries of *non-circular*

† In instances where the time of fall of the sphere was sufficiently long to allow leisurely observation, it was possible to correlate these 'dips' visually with off-axis motion.

‡ The experiments of Karnis, Goldsmith & Mason (1966) show that, when inertial effects are sensible, a sphere released near the tube wall in a quiescent fluid migrates permanently to the tube axis due to the action of an inertial lift force associated with the asymmetry of the flow field (Brenner 1966; Cox & Brenner 1968). Clearly, this is due to a conventional wall effect, and will therefore vanish in the limit as $a/R_0 \to 0$, keeping b/R_0 fixed. Hence the extent of radial migration in a tube of given length can be made as small as desired by choosing a/R_0 sufficiently small, at least in principle.

cross-section. For the general case of a conduit of arbitrary cross-section, theory (Brenner 1962) predicts that

$$\Delta PA/D = v_0/V_m, \tag{6}$$

where A is the cross-sectional area of the cylinder, and v_0 is the approach velocity to the particle when fluid flows in laminar flow through the duct at mean velocity V_m.† Thus, for example, in place of (1), we have that $\Delta PA/D = 2{\cdot}093\ldots$ for a particle located at the axis of a square duct; similarly, $\Delta PA/D = 22/9$ for a particle at the axis of a duct of equilateral triangular cross-section. Equation (6) does not require that the particle be spherical; rather, it applies to particles of any shape, provided that, if any lateral forces act upon the particle, D refers only to that component of the vector force which lies parallel to the cylinder walls.

Referring to figure 4, it appears that the apparent constancy of the $\Delta PA/D$ ratio for $Re < 125$ may not merely be an asymptotic result, valid only as $Re \to 0$, in the sense, say, that Stokes law is an asymptotic result; rather, it is possible that the limiting value of $Re \approx 125$ may correspond to a true transition point. In this connexion it is of interest to note that $Re \approx 130$ is the point at which the flow pattern behind the sphere first becomes unsteady (Taneda 1956; Torobin & Gauvin 1959).

Since the theory (Brenner 1962) is strictly applicable only for small ratios of particle to duct size, the transition point in a plot of $\Delta PA/D$ *vs.* Re for particles and ducts of any shapes ought only to depend upon the geometric shape (and orientation) of the particle, but not upon the configuration of the cylinder. If this is indeed true it follows that the transition point for a spherical particle would always be $Re \approx 125$, irrespective of the cross-sectional shape of the cylindrical duct in which it fell.

In contrast to the possibly sharp transition occurring at the Reynolds number where a steady flow pattern ceases to be stable, the other limiting result, $\Delta PA/D = 1{\cdot}0$, observed at $Re > 6000$, is almost certainly an asymptotic result, strictly valid only in the limit where $Re \to \infty$. Since the cylinder walls experience no net force for this case, and since they lie at an effectively infinite distance from the particle, it seems improbable that an extension of the experiments to Reynolds numbers substantially above those investigated here would reveal any further $\Delta PA/D$ 'transitions'.

The simple, idealized model of a *point force* of strength D directed along the axis of a circular tube of radius R_0 furnishes insight into the remarkable nature of the phenomenon with which we are dealing in these experiments.‡ Elementary dimensional arguments show that the force on the wall is necessarily of the functional form

$$F_w/D = \text{function } (D/\rho\nu^2), \tag{7}$$

† For example, for Poiseuille flow in a circular tube,

$$v_0/V_m = 2[1-(b/R_0)^2].$$

‡ In this connexion it is of interest to note that an *exact* solution of the complete Navier–Stokes equations is available (Landau & Lifshitz 1959) for a point force in an *unbounded* fluid.

where $D/\rho v^2$ plays the role of a generalized Reynolds number. The pressure drop is not an independent parameter since it is related to F_w and D via (3). What is paradoxical about (7) is that the force on the wall is independent of the tube radius, despite the significant influence of tube radius on the far-field velocity distribution, which in turn governs the magnitude of this wall force.

This research was supported by grants from the National Science Foundation (grant nos. GK-56 and GK-1458) and the National Aeronautics and Space Administration under research grant NGR-33-016-167 to New York University.

The UCON fluid employed in the experiments was kindly donated by the Union Carbide Chemical Company.

REFERENCES

BRENNER, H. 1962 Dynamics of a particle in a viscous fluid. *Chem. Engng Sci.* **17**, 435.

BRENNER, H. 1966 Hydrodynamic resistance of particles at small Reynolds numbers. Chapter 5 in *Advances in Chemical Engineering, Volume* 6 (T. B. Drew, J. W. Hoopes and T. Vermeulen, eds.), pp. 340, 396. New York: Academic Press.

COX, R. G. & BRENNER, H. 1968 The lateral migration of solid particles in Poiseuille flow: Part 1. Theory. *Chem. Engng Sci.* (in the Press).

FELDMAN, G. A. 1967 Experiments on the pressure drop created by a sphere settling in a liquid at Reynolds numbers up to 20,000. Ph.D. dissertation, New York University, Bronx, New York.

FIDLERIS, V. & WHITMORE, R. L. 1961 Experimental determination of the wall effect for spheres falling axially in cylindrical vessels. *Br. J. Appl. Phys.* **12**, 490.

HABERMAN, W. L. & SAYRE, R. M. 1958 Motion of rigid and fluid spheres in stationary and moving liquids inside cylindrical tubes. *David Taylor Model Basin Rept.* no. 1143, U.S. Navy Dept., Washington, D.C.

KARNIS, A., GOLDSMITH, H. L. & MASON, S. G. 1966 The flow of suspensions through tubes: V. Inertial effects. *Canad. J. Chem. Engng.* **44**, 181.

LANDAU, L. D. & LIFSHITZ, E. M. 1959 *Fluid Mechanics*, p. 86. Reading, Massachusetts: Addison-Wesley.

LAPPLE, C. E. & SHEPHERD, C. B. 1940 Calculation of particle trajectories. *Industr. Engng Chem.* **32**, 605.

MAXWORTHY, T. 1965 Accurate measurements of sphere drag at low Reynolds numbers. *J. Fluid Mech.* **23**, 369.

MCNOWN, J. S., LEE, H. M., MCPHERSON, M. B. & ENGEZ, S. M. 1948 Influence of boundary proximity on the drag of spheres. *Proc. 7th Intern. Congr. Appl. Mech., London 1948*, Vol. 2, Part I, p. 17. (Reprinted as State University of Iowa Reprints in Engineering, Reprint 81, Iowa City, Iowa.)

PERRY, J. H. 1963 (editor) *Chemical Engineers' Handbook*, 4th edition, pp. 3–70 and 3–201. New York: McGraw-Hill.

PLISKIN, I. & BRENNER, H. 1963 Experiments on the pressure drop created by a sphere settling in a viscous liquid. *J. Fluid Mech.* **17**, 89.

TANEDA, S. 1956 Experimental investigation of the wake behind a sphere at low Reynolds numbers. *J. Phys. Soc. Japan*, **11**, 1104.

TOROBIN, L. B. & GAUVIN, W. H. 1959 Fundamental aspects of solids-gas flow. Part II. The sphere wake in steady laminar fluids. *Canad. J. Chem. Engng.* **37**, 167.